A + B → B Reaction for Unequal Reactant Concentrations

Panagiotis Lianos

School of Engineering, University of Patras, 26500 Patras, Greece

Panos Argyrakis*

Department of Physics, University of Thessaloniki, 54006 Thessaloniki, Greece

*Received: January 3, 1994; In Final Form: April 27, 1994**

We have studied the reaction A + B → B ([A] ≪ [B]) by computer simulations in 3-, 2-, and 1-dimensional lattices. We first reviewed the case of normal homogeneous lattices and then extended the study to lattice clusters below, at, and above the critical percolation threshold. The decay profiles of the minority species A were analyzed by a model of stretched exponentials of the form: $I(t) \approx \exp(-C_1 t^f + C_2 t^{2f} - ...)$. The corresponding reaction rate is then time-dependent. The analysis of the simulated decay profile was better when a higher number of terms of the series were employed. Higher-order terms are necessary when the reaction domain is more restricted. The choice of the approximation order mainly affects the calculated value of the reaction rate at long times. The exponent f was smaller when the reaction domain was more restricted, i.e., below the percolation threshold or at smaller dimensionalities. The above reaction is a model for time-correlated fluorescence quenching analyses. We compared these results with experimental data from time-resolved fluorescence measurements on pyrene decanoate incorporated in lipid vesicles (recorded with the photon counting technique), and we found that only two terms in the above stretched-exponential expression suffice to satisfactorily describe the fluorescence decay profile. The present work is useful for applications to fluorescence probing of organized molecular assemblies.

1. Introduction and Theory

Chemical reactions in restricted spaces have been the focus of a large number of studies in the past decade, as it was revealed that the usual kinetic laws do not hold anymore, and one has to resort to a fractal picture, or more generally, to a power law with noninteger dimensionality, even for the simplest of the reactions.[1] The bimolecular reaction A + B → B is in this category, but most studies to the present day deal with the case of equal initial reactant concentrations ([A] = [B]). However, the case of the reaction A + B → B ([A] ≪ [B]) is also of great importance since, among others, it represents the reaction between an excited fluorophore and a quencher. Fluorescence quenching experiments[2] have been and are extensively used as a valuable tool to probe both structure and dynamics of microheterogeneous systems such as micelles, microemulsions, lipid vesicles, and polymers. The analysis of fluorescence quenching is, in most of the cases[2] time-resolved. Different models have been used to interpret the fluorescence decay profiles. Thus, in the case of micelles and microemulsions, the quenching reaction is best described by the interaction between compartmentalized reactants, which are distributed among the available micelles.[3,4] Such a model cannot be easily extended to lipid vesicles or biological supramolecular assemblies which are large and fairly complex systems. There have been several approaches to treat the fluorescence quenching reaction in lipid vesicles. The vesicle lipid phase behaves as a two-dimensional viscous fluid. Thus, an attempt has been made to describe fluorescence quenching kinetics in vesicles by the Smoluchowski diffusion theory.[5,6] This theory implies a time-dependent reaction rate and a stretched exponential fluorescence decay law, i.e., square root of time dependence. This type of dependence on time is a consequence of the fact that the dimensionality of the reaction domain is considered Euclidean (integer). In addition to this limitation, a complication arises by the finding that the reacting species might be aggregated in the vesicle lipidic core, particularly, in the vesicle gel phase,[7] so that (quenching) reaction might not be purely diffusion-controlled. Thus, other authors analyzed the fluorescence decay profile by a sum of several exponential terms.[6-8] Of course, it is true that any fluorescence decay profile can be fitted by a sum of several exponential terms. The reliability of fitting procedures has been recently increased by using global analysis[9] or maximum entropy analysis.[10] However, a sum of exponentials cannot give a close form expression for the reaction rate. Furthermore, it cannot give direct information on the structure of the reaction domain. We believe that all these difficulties stem from the fact that all models used so far do not involve the notion of dimensionality. However, microheterogeneous phases are essentially systems of restricted geometry. For this reason models describing reactions in such media must include a parameter related to the dimensionality of the reaction domain.

The most fundamental quantity necessary to describe the kinetics of a chemical reaction is the rate constant. Experimentally, one observes the evolution of the monitored reacting species, and with the help of a kinetic model the rate constant is calculated. In cases of fluorescence probing, where an excited fluorophore is quenched by a quencher, the evolution of the reaction is monitored by fluorescence. Then, analysis of the flurescence decay profile gives the quenching rate constant. However, it is now well understood that constant rates only exist in a small part of the known kinetics, while spatial or energetic disorder leads to time-dependent constants. This is the case of fluorescence quenching in organized molecular assemblies, such as micelles, microemulsions, and vesicles which consist of microdomains; i.e., they possess geometrical disorder. Fluoresence quenching in liquid media can generally be analyzed in two parts. One part is the energy exchange between the excited and the quenching species. Energy can be transferred to a distance r by dipole or multipole interactions with probability obeying a power law $1/r^s$, where $s = 6, 8, 10$, etc., for dipole–dipole, dipole–quadrupole, quadrupole–quadrupole, etc., interactions, respectively.[11,12] Also, energy can be transferred by electron transfer with probability proportional to $\exp(-kr)$, where k is a constant. In most cases the employed fluorescence quenching couples are such that no important transfer occurs when they are immobilized. The probability of a transfer can then be satisfactorily represented by a power law with large

* Abstract published in *Advance ACS Abstracts*, June 15, 1994.

0022-3654/94/2098-7278$04.50/0

s values. The second part of fluorescence quenching in fluid media is a diffusion-controlled process. Allinger and Blumen[13] have derived a general equation for reactions occurring by both energy transfer and diffusion, using a power law for the transfer probability. Thus, the survival probability of the decaying fluorescent species, represented by the time-dependent fluorescence intensity $I(t)$, is given (in a simplified form) by

$$I(t) \approx \exp(-At^{\Delta/s} + \sum_{n=1}^{\infty} B_n D^n t^{n-2n/s+\Delta n/s}) \quad (1)$$

where Δ is the dimensionality of the reaction domain, D is the mutual diffusion coefficient, and A and B_n are constants depending on Δ and the occuration probability p of the available solubilization site by quenchers (assuming that quenchers are much more numerous than excited fluorophores). Analytical expressions for B_n are given in ref 13. This equation, which is derived by ensemble averaging over all quenching possibilities, clearly separates the two parts of the interaction. Note that if Δ/s is a small number, as in the case of multipole interactions, then $At^{\Delta/s}$ corresponds to a rapidly decaying contribution. This practically implies that long-range transfer is negligible. Only close-lying reactants can interact. Since reactants can come close by diffusion, then only the diffusion-controlled part of the interaction, i.e., the infinite series of eq 1, is important. On the other hand, for immobile reactants ($D = 0$) the only contribution is the energy-transfer term $At^{\Delta/s}$. Diffusion-controlled reactions in media with geometrical restrictions should then be modeled by the infinite series of eq 1.

Equation 1 is too complicated for practical applications. However, an alternative form can be employed by using a cumulant expansion introduced by Blumen, Klafter, and Zumofen[14-16] to describe energy migration by random walk in lattices with spatial disorder. In terms of cumulants, the decay law becomes[16,17]

$$I(t) \approx \exp\sum_{i=1}^{\infty} \kappa_i(t)\frac{(-\lambda)^i}{i!} \quad (2)$$

where $\kappa_i(t)$ are the cumulants, $\lambda = -\ln(1 - p)$, and p is the occupation probability. It is known[17] that, for any distribution of the reaction probabilities and for a given value of time t, $\kappa_1(t)$ is equal to the mean $\mu(t)$, and $\kappa_2(t)$ is equal to the variance. The reaction rate is determined by the parameter of the number of distinct sites $S(t)$ visited by the random walker within time t. Then $\kappa_1(t)$ is proportional to the mean of $S(t)$ and $\kappa_2(t)$ to its variance. Higher-order cumulants are more complicated expressions,[17] also involving $S(t)$. However, we should note that even though in a regular lattice $S(t)$ might be proportional to t, in lattices with spatial disorder[16] $S(t) \approx t^f$ where $0 < f < 1$. It is then obvious that the successive cumulants introduce successive powers of t into the decay law, with exponents being integral multiples of f. Therefore, the decay law can be written as

$$I(t) \approx \exp(-C_1t^f + C_2t^{2f} - C_3t^{3f} + ...), \quad 0 < f < 1 \quad (3)$$

where f, C_1, C_2, C_3, etc., are constants. It is also obvious that C_1 should be related with λ, C_2 with λ^2, etc. This simplified decay law is now useful for practical applications if an important question is answered: are the C's related with each other? Inspection of eq 2 shows that the question is reduced to whether the cumulants $\kappa_i(t)$ are correlated. There are discrete distributions,[17] like the Poisson or the binomial distribution, where the κ's are given by specific relations. In the most common case, the normal (Gaussian) distribution, the first cumulant is equal to the mean and the second to the variance, which are not related, while all higher-order terms are zero.[17] Fluorescence decay profiles recorded by the photon counting technique, thus containing noisy data, correspond to normal distribution. Such profiles should be described by the following equation

$$I(t) \approx \exp(-C_1t^f + C_2t^{2f}), \quad 0 < f < 1 \quad (4)$$

where C_1 and C_2 do depend on λ (i.e., reactant concentration), but they are also influenced by dispersion, defined by the physical system itself. Therefore, they are not correlated. If the distribution of the reaction probabilities is not normal, then C_3 and higher-order terms might be different from zero and the C's might be correlated. This question will be one of the subjects of the present work. When the reaction domain is self-similar (fractal), then f is proportional to the fractal dimension of the reaction domain. It is then obvious that the decay law of eqs 3 and 4, which are combinations of stretched exponentials, describe a specific dependence on both the reactant concentration (through λ) and geometry (through f). The reaction rate can be now easily derived from eq 3 (or eq 4) by differentiation[18]

$$K(t) = fC_1t^{f-1} - 2fC_2t^{2f-1} + ... \quad (5)$$

This expression gives a first-order rate which, of course, is time-dependent, as expected.

It is obvious from the above theory that the fluorescence decay profile and the rate constant for diffusion-controlled quenching in a geometrically disordered medium should be expressed as a series of terms containing noninteger powers of time. We have experimentally found that in some cases only one term of the series suffices to fit the experimental decay profile.[19] In other cases, two terms are necessary[18,19] and may be other cases where three or more terms might be needed, as described above. To clarify this question, we have undertaken the present work where the A + B → B ([A] ≪ [B]) reaction is studied by computer simulations in one-, two-, and three-dimensional lattice clusters, which are supposed to satisfactorily represent organized molecular assemblies.

In order that a microheterogeneous system, e.g., vesicles, is represented adequately by a fractal picture, it should possess the property of self-similarity. It is true that perfect fractals can be produced only on a computer screen, but any disordered system may show some degree of self-similarity, and such an assumption is amenable to confirmation by experiment. At any rate, it is well-known that these structures are highly ramified, and thus a structure similar to a percolation cluster may be a reasonable model to explore.

2. Computational Methods

The techniques used to perform the computer simulation for the fluorescence-quenched reactions were similar to these previously reported.[24] Briefly, clusters are generated on a lattice with a specified dimensionality with size $L = 1\,000\,000$ (1-D), $L = 1000 \times 1000$ (2-D), and $L = 100 \times 100 \times 100$ (3-D) sites. The clusters are generated using the techniques of the percolation problem by specifying the probability p for an open site, which in this work varies, depending on the dimensionality and the case examined. For some cases the largest cluster is isolated and further used, while for others all clusters of all sizes are taken into account. The cluster characterization is done using the cluster multiple labeling technique. The reaction is simulated by positioning a certain number of A and B particles on the available clusters at time $t = 0$. Reaction proceeds in the known way: all particles perform random walks with the stipulation that when it is found that an A and a B particle occupy the same site, then A is removed from the system but B stays in the same site. This situation depicts the collision between an A and a B particle leading directly to a reaction. When two A or two B particles collide, nothing happens. We use exclusion volume principle; i.e., we do not allow more than one particle to occupy simultaneously the same site. We monitor the concentration [A] of A particles (i.e., the minority

TABLE 1: Reaction Rate Constant vs Total Number of Species B in a Homogeneous 3-D Lattice

$[B] \times 10^{-3}$	K (10^6 s^{-1})[a]	$k \times 10^9$	$[B] \times 10^{-3}$	K (10^6 s^{-1})[a]	$k \times 10^9$
1	1.3	1.3	4	5.2	1.3
2	2.6	1.3	5	6.7	1.3
3	3.9	1.3	10	14	1.4

[a] Units of inverse time have been assigned to the values of K by assuming each random step to be equal to 1 ns, a value very close to real times in fluorescence probing.

species representing the excited fluorophore) as a function of time. The basis for our time unit is one Monte Carlo step (MCS), which is defined as the time it takes for a particle to move to its nearest neighbor. In the present calculation time changes from 0 to 300. If we assume that 1 MCS is equivalent to the time order of nanoseconds, then the real situation of fluorescence decay is nicely represented by the present simulation. We have monitored several interactions by varying the number density of B. It should be underlined that, by assuming a uniform time distribution and by making all available sites equivalent, no time dispersion and no energetic dispersion have been taken into account. Thus, the analysis focuses at purely dimensionality considerations.

3. Results and Discussion

The A + B → B ([A] ≪ [B]) Reaction in a Homogeneous 3-, 2-, and 1-Dimensional Lattice. When a minority species A interacts with a majority species B in a nonreversible reaction which is carried out in a nonrestrictive environment, then the kinetics of the reaction obeys the following simple differential equation:

$$d[A]/dt = -k[B][A] \tag{6}$$

the solution of which is

$$[A](t) = [A]_0 e^{-k[B]t} \tag{7}$$

where [A] and [B] are either the molar concentrations or the number densities of the corresponding reactants. k then is a constant, the second-order reaction rate constant. We have started our study of the above reaction by first simulating it in a homogeneous three-dimensional lattice. The decay of the species A vs time was described by a single-exponential function in accordance with eq 7. Table 1 shows the calculated values of the corresponding first-order rate constant $K = k[B]$, as well as the quotient of $K/[B]$, i.e., the value of k. In Table 1, [B] is the global number density of the B species found by division of the absolute number of B by 1 000 000 (the total number of lattice points).

We then note that not only the decay obeys eq 7, i.e., k is a constant, but it is also unaffected by [B], within a reasonable range of [B] values. Indeed, the number of our lattice points was 10^6 (100 × 100 × 100 lattice). The number density of A was $10^2/10^6$, i.e., only 0.01%, while the maximum number density [B] was only $10^4/10^6$, i.e., 1% of the total number of lattice points. At higher B densities, however, the kinetics did not obey eq 7 anymore. This was expected, since the lattice size is then two small for such high reactant densities. Even for [B] = 0.01, a deviation of k from the calculated value 1.3×10^9 has already been observed. In another series of simulated reactions we used [A] = 0.001 and [B] ≥ 0.04. We have then found that the decay of A does not obey eq 7; i.e., it is no more a single-exponential function of time. This finding is obviously due to the fact that the concentration of the reacting species is too large for the lattice space used, which is a manifestation of finite size effects. Obviously, a restricted reaction does not obey eq 7. This finding was further verified by carrying out reactions in a homogeneous 2-D and a homogeneous 1-D lattice of the same reactant to lattice point ratios, i.e., [A] = 0.0001, [B] = 0.001–0.01, and 10^6 lattice points (1000 × 1000 for 2-D and 1 000 000 for 1-D). In both cases, we have found that the reaction did not obey eq 7. When the decay of A is not a single-exponential function of time, this is equivalent to saying that the reaction rate is not constant any more. Geometrical restrictions, either in space or in dimensionality, then impose reaction rates which are time-dependent. The difference in the kinetics of the reactions for the same reactant number density, but different lattice dimensionality is seen by the semilogarithmic plots of the decay profiles of A shown in Figure 1.

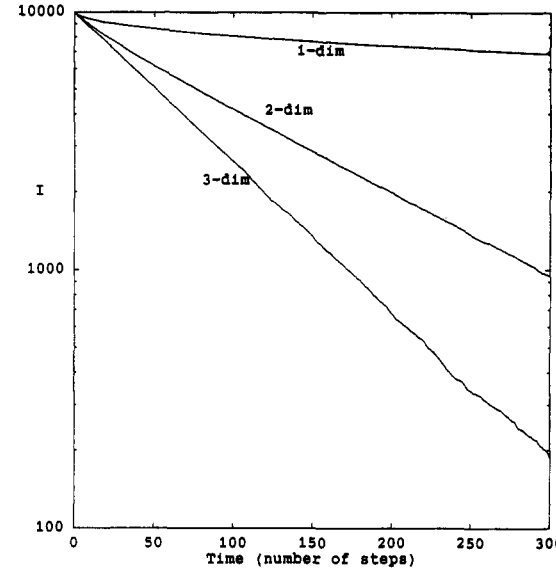

Figure 1. Decay of [A] vs time for a 3-D, 2-D, and 1-D lattice of size 1 000 000. [A] = 0.0001 and [B] = 0.01 in all three cases.

3-Dimensional Lattices at and below the Percolation Threshold. We simulated the above reaction in a 3-D lattice (100 × 100 × 100) at the percolation threshold (fraction of allowed sites p = 0.312) and below the threshold (p = 0.25). [A] was always equal to 0.0001, and [B] varied from 0.001 to 0.01. Both A and B were placed on allowed sites and were forced to make random steps only within the allowed clusters. In the case of p = 0.312 we have carried out the analysis in two different cases: (1) only the largest cluster was allowed, while all smaller clusters were erased, and (2) all clusters were allowed. The latter is more close to real situations in fluorescence probing of organized molecular assemblies. In the case of p = 0.25, all clusters were allowed. In all three cases the decay profiles of [A] were not described by eq 7; i.e., they were not single exponentials. Obviously, the decay rate was then time-dependent. We tried to fit the simulated decay profiles of [A] by eq 1, in the form of eq 3, using subsequent order approximations, i.e., increasing number of terms inside the exponential. The quality of fit was judged by visual inspection and by the distribution of the residuals, i.e., the differences between the decay data and the fitted values at each random step (at each time value). As seen in Figure 2, fitting was better when a higher number of terms inside the exponential were used. The improvement of the quality of fit was more marked at higher [B] values. Both these findings were expected, since with the increase of terms the approximation of the infinite series is improved and also, since their importance increases as [B] increases. We have thus found that in these computer-generated decay profiles the constants C_3, C_4, etc., are not zero. According to the theory presented above, this suggests that the distribution of the number of distinct sites visited by the random walker within a given time is limited by the existence of a lower limit for $S(t)$, (i.e., zero, since no negative values are allowed) and also the existence of an upper limit (i.e., equal number of visited sites as the number of random steps) and the Gaussian becomes skewed. Furthermore, the diversion from a perfect Gaussian, obviously, creates a certain degree of correlation between the C_i values so that fitting with

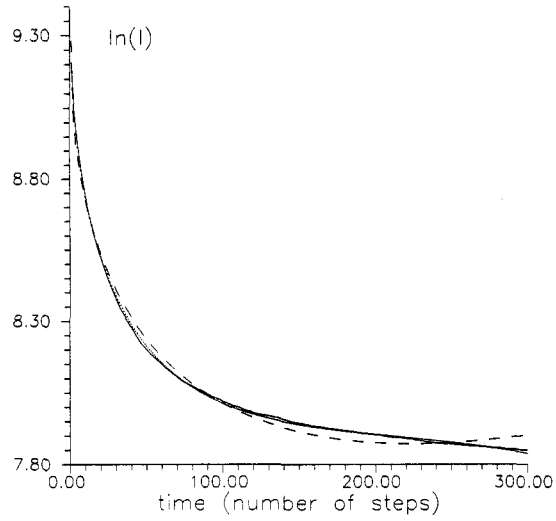

Figure 2. Computer generated (—) and fitted curve using (- - -) eq 4 amd (• • •) eq 8.

many terms produces ambiguous, nonreproducible parameter values. In Table 2 we present values of the obtained parameters by fitting eq 3 to the decay profiles of [A]. We have used two different approximation cases, i.e., eq 4 ($C_2 \neq 0$, $C_3 = 0$) and the following eq 8 ($C_3 \neq 0$):

$$I(t) \approx \exp(-C_1 t^f + C_2 t^{2f} - C_3 t^{3f}), \quad 0 < f < 1 \qquad (8)$$

The fittings obtained with eq 4 were unique. Those obtained with eq 8 were nonunique. For this reason we have made a choice of the values of f and let only the C's vary, when eq 8 was employed. By fitting eqs 4 and 8 to the decay profiles of [A], we calculated f, C_1, and C_3 (when necessary) which were then introduced into eq 5 to obtain the values of $K(t)$. For practical reasons and in order to present the evolution of K with time, we have chosen to tabulate K_1, the value of $K(t)$ at the beginning of the reaction, K_L, the value of $K(t)$ at the end of the reaction, and K_{AV}, the average value over 300 steps. In Table 2 we then present the calculated values of f, K_1, K_L, and K_{AV} as well as the ratio C_2/C_1 (and C_3/C_1 when necessary) which shows the importance of the higher-order approximation, in relation to the first-order term.

The f values, calculated with eq 4, shown in column 2 of Table 2, were not affected by the population of species B. Thus, the values of f, calculated with eq 8, were also chosen to be independent of [B]. f was found smaller when the reaction domain was more restricted, i.e., for $p = 0.25$. f was the largest when the reaction was carried out exclusively in the percolation cluster. Higher-order approximation is more important when the environment is more restricted. Thus, both C_2 and C_3, shown in columns 3 and 4 of Table 2, obtained higher values with respect to C_1 when $p = 0.25$. Furthermore, C_2 and C_3 became more important when [B] was larger. This is in accordance with the above theory which suggests that (other factors kept constant) C_i is proportional to λ^i (where $\lambda = -\ln(1-p)$). It is also in accordance with previous experimental findings showing the same quencher concentration effect.[19] C_2/C_1 was found larger when eq 8 was used in the place of eq 4. This is a purely computational effect since in the case of eq 8 the added C_2 is increased to counterbalance the subtracted C_3. The rest of the columns in Table 2 give the values of the first-order rates K. Naturally, all K's increased with [B], since the first-order reaction rate is higher when the reactant population is higher. K_1 was always larger than K_L as it always happens with this type of reactions. K_{AV}, naturally, obtained an intermediate value. K_1 was relatively small in the more restricted domains, i.e., for $p = 0.25$ or for $p = 0.312$ when all clusters were allowed. K_1 was much higher when the reaction was done exclusively within the largest cluster at the percolation threshold. The effect of the geometrical restrictions was even more marked in the values of K_L. K_L was negligible when $p = 0.25$, was very small when $p = 0.312$ with all clusters allowed, and became large when the reactants were free to move within the percolation cluster. Thus, in the less restricted environment the rates are higher both at early and at long reaction times. The K_{AV} values were affected to a rather limited extent when eq 8 was used in the place of eq 4. The effect was higher for K_1, especially, in the percolation cluster, while K_L was found, dramatically, different with eq 8 from with eq 4, especially, in the percolation cluster. It is then obvious that the proper approximation plays a very important role for the calculation of the long-time reaction rates. This role

TABLE 2. Values of f, C_2/C_1, C_3/C_1, K_1, K_L, and K_{AV} for a Three-Dimensional Lattice at and below the Percolation Threshold

10^{-3}[B]	f	$10^3 C_2/C_1$	$10^3 C_3/C_1$	K_1	K_L	K_{AV} (10^6 s^{-1})[a]
		$p = 0.312$ (percolation threshold), all clusters allowed, analysis with eq 4				
1	0.55	11		1.8	0.07	0.21
5	0.55	15		9.7	0.24	0.87
10	0.56	17		18	0.31	1.6
		$p = 0.312$ (percolation threshold), all clusters allowed, analysis with eq 8				
1	0.55	12	0.0	2.1	0.07	0.21
5	0.55	18	0.1	10	0.26	0.88
10	0.55	19	0.1	19	0.35	1.6
		$p = 0.312$ (percolation threshold), only the largest cluster allowed, analysis with eq 4				
1	0.57	12		20	0.7	2.0
5	0.56	17		87	1.2	7.2
10	0.56	21		156	2.0	11
		$p = 0.312$ (percolation threshold), only the largest cluster allowed, analysis with eq 8				
1	0.67	16	0.1	16	0.9	2.0
5	0.67	21	0.2	74	3.3	7.5
10	0.67	27	0.3	143	7.5	12
		$p = 0.25$ (below percolation threshold), all clusters allowed, analysis with eq 4				
1	0.43	34		2.2	0.02	0.11
5	0.46	34		9.8	0.04	0.51
10	0.44	39		20	0.05	0.94
		$p = 0.25$ (below percolation threshold), all clusters allowed, analysis with eq 8				
1	0.44	48	0.9	2.3	0.02	0.12
5	0.44	49	0.8	11	0.06	0.52
10	0.44	59	0.7	21	0.09	0.96

[a] See footnote to Table 1.

TABLE 3: Values of f, C_2/C_1, C_3/C_1, K_1, K_L, and K_{AV} for a Two-Dimensional Lattice at and below the Percolation Threshold

10^{-3}[B]	f	$10^3C_2/C_1$	C_3/C_1	K_1	K_L	K_{AV} (10^6 s^{-1})[a]
		p = 0.5931 (percolation threshold), all clusters allowed, analysis with eq 4				
1	0.55	14		2.0	0.06	0.19
5	0.55	15		9.7	0.25	0.88
10	0.57	14		18	0.46	1.7
		p = 0.5931 (percolation threshold), all clusters allowed, analysis with eq 8				
1	0.55	14	0.0	2.0	0.06	0.19
5	0.55	20	0.2	10	0.29	0.89
10	0.55	15	0.0	19	0.49	1.7
		p = 0.5931 (percolation threshold), only the largest cluster allowed, analysis with eq 4				
1	0.58	13		6.5	0.21	0.64
5	0.58	14		29	0.63	2.8
10	0.58	15		53	0.83	4.8
		p = 0.5931 (percolation threshold), only the largest cluster allowed, analysis with eq 8				
1	0.67	17	0.1	5.3	0.29	0.64
5	0.67	18	0.1	25	1.0	2.8
10	0.67	18	0.1	46	1.7	4.9
		p = 0.5 (below percolation threshold), all clusters allowed, analysis with eq 4				
1	0.49	23		1.8	0.02	0.12
5	0.44	27		9.5	0.14	0.57
10	0.44	29		18	0.22	1.1
		p = 0.5 (below percolation threshold), all clusters allowed, analysis with eq 8				
1	0.44	28	0.0	2.1	0.03	0.13
5	0.44	40	0.8	10	0.16	0.59
10	0.44	40	0.6	20	0.26	1.1

[a] See footnote to Table 1.

TABLE 4: Values of f, C_2/C_1, K_1, K_L, and K_{AV} Found with the Help of Eqs 4 and 5 (C_3 = 0) for a One-Dimensional Lattice at 100% and 90% of Allowed Sites

10^{-3}[B]	f	$10^3C_2/C_1$	K_1	K_L	K_{AV} (10^6 s^{-1})[a]
		100% Allowed Sites			
1	0.51	0	1.1	0.07	0.12
5	0.55	4	4.7	0.30	0.58
10	0.51	1	11	0.63	1.2
		90% Allowed Sites			
1	0.36	60	1.4	0	0.05
5	0.37	65	6.8	0	0.22
10	0.36	67	14	0	0.43

[a] See footnote to Table 1.

TABLE 5: Values of f, C_2/C_1, K_1, K_L, and K_{AV} Found with the Help of Eqs 4 and 5 for Three-Dimensional Lattice above the Percolation Threshold ([A] = 0.0001 and [B] = 0.01)

density of allowed clusters	f	$10^3C_2/C_1$	K_1	K_L	K_{AV} (10^6 s^{-1})[a]
0.312	0.56	17	18	0.3	1.6
0.32	0.56	17	20	0.4	1.7
0.35	0.60	12	19	0.6	2.1
0.40	0.65	7	19	1.2	2.8
0.50	0.83	2	14	2.8	5.0
0.60	0.90	2	14	3.5	6.5
1.0	1.0		14	14	14

[a] See footnote to Table 1.

is even more important in environments where the long-time reaction probability is higher.

2-Dimensional Lattice at and below the Percolation Threshold. A similar analysis was carried out in a 2-D lattice (1000 × 1000) at the percolation threshold (p = 0.5931) and below the threshold (p = 0.50). The results are tabulated in Table 3. As in Table 2, the analysis was carried out with eq 4 and with eq 8. The results were qualitatively the same for both three and two dimensions. The quantitative differences are not extensive either. Thus, f was found to have the smallest value below the percolation threshold C_3/C_1 were also found to have the largest value below the threshold. We then verified that the choice of the right approximation order is more important below the percolation threshold. The K's also varied in the same manner here as in the three-dimensional lattice both at and below the threshold. We might then safely propose that in computer simulations of the above reaction 2-D and 3-D lattices give results with rather unimportant differences, as long as the ratio of the number of the reactants over the number of allowed sites remains equivalent. This is expected, since the spectral dimension that determines the reaction rate is about the same for 2-D and 3-D percolation clusters.

1-Dimensional Lattice at 100% and 90% of Allowed Sites. Finally, a similar analysis was carried out in a one-dimensional lattice (1000000 points) at 100% and 90% allowed sites. The results are tabulated in Table 4. The analysis was made with both eq 4 and 8. However, it was found that analysis made with eq 8 did not add any new information. So the corresponding data are not shown.

As in three and two dimensions, the data were modified when going from the less restricted to the more restricted lattice. Thus, f and the K's take smaller values in 90% than in 100% allowed space. Also, C_2/C_1 increases very much in going to the more restricted space. So there is an analogy of the data obtained in one-dimensional lattice with those obtained in the higher-dimensional lattices. Note, in this respect, the substantial progressive decrease of f with decreasing dimensionality from p = 0.25 (3-D) to p = 0.90 (1-D).

Progressive Variation of Restrictiveness in a 3-Dimensional Lattice. In another series of simulated reactions we have used the same above 3-D lattice, but we have varied the percentage p of allowed sites. The number of A species was fixed to 100 and that of the B species to 10 000. We have analyzed the obtained decay curves with eq 4. The results are shown in Table 5. We have found that f progressively decreased from f = 1 (that corresponds to homogeneous lattice) to f = 0.56 (that corresponds to the percolation threshold) as p decreased. As expected, C_2/C_1 increased and the K's decreased with decreasing p, i.e., with increasing restrictiveness of the reaction domain. f was smaller than the value expected at the percolation threshold according to the Alexander Orbach conjecture.[21] This is simply due to the order of approximation used. Note also the progressive decrease of the importance of C_2 with respect to C_1 as f increases, i.e., as the restrictions of the reaction domain are relaxed. At f = 1 (homogeneous space) $K_1 = K_L = K_{AV}$. As the restrictions increase,

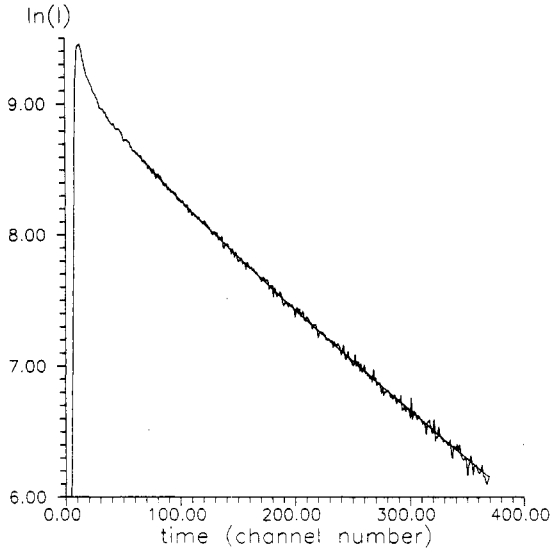

Figure 3. Fluorescence decay profile of 4×10^{-5} M pyrenedecanoate in 2×10^{-4} M vesicle forming cardiolipine.

K_L and K_{AV} progressively decrease while K_1 increases to obtain the value found at the threshold.

Comparison with Experimental Results. Equation 4 has been successfully applied to describe fluorescence decay profiles in several cases of fluorescence probing of water-in-oil microemulsions and lipid vesicles.[18,22-27] In all cases, an excellent fit was obtained (ef Figure 3) using either $C_2 \neq 0$ or even $C_2 = 0$.[19] We have never succeeded to fit eq 8 to experimental decay profiles recorded with the photon-counting technique, i.e., with a technique producing noisy data. This fact comes in verification of the above assertion that (noisy) experimental data better approach a normal (Gaussian) distribution of values of the fluorescence intensity at each time t, so that in a cumulant expansion only the first and the second term have nonzero values. It is useful to comment on the values of f, C_2/C_1, K_1 K_L, and K_{AV} obtained in various experimental cases as compared with the present simulation data. f has been found to vary in a rather large range of values, of course, being always smaller than unity. The efficiency of a reaction in organized molecular assemblies directly reflects on f. Thus, efficient localized interactions, which can be designated as quasi-static interactions, correspond to very low f values. Diffusion-limited interactions correspond to higher f values. As in simulated interactions, f values cannot be uniquely related with the geometry of the reaction domain. Nevertheless, restricted geometries yield low f values in the sense that reactions are then more localized (smaller number of distinct sites visited for the same number of random steps). The ratio C_2/C_1 goes to the opposite direction. Thus, they are larger in more restricted geometries and at higher B concentrations. Furthermore, we have found that, in experimental situations, there is an important role played by the efficiency of the reaction in relation with the duration of the lifetime τ_0 of the excited state of the fluorophore. Thus, C_2/C_1 is larger when τ_0 is smaller.[20] The K's behave in a similar manner as in simulated interactions. K_{AV} gives a value which represents well the overall efficiency of the interaction. K_1 gives the reaction probability at short times and K_L at long times. Efficient localized interactions correspond to large K_1 values, while efficient diffusion corresponds to large K_L values. The difference between K_1 and K_L is larger when f is smaller.

4. Conclusions

In this work we carried out computer simulation for the A + B reaction for the case of unequal initial concentrations of the A and B reactants. We covered the three usual dimensionalities, i.e., 1-D, 2-D square, and 3-D simple cubic, and also extended the work to lattice clusters built using the percolation model, at the critical point and above and below it. In this way we tried to cover several possible degrees of inhomogeneity of the reaction space and draw the corresponding conclusions. Our results show that the decay of the minority species follows a stretched exponential form, where the exponent is characterized by a "spectral dimension", which is a generalized form of a fractal dimension. The calculations indicate that this exponent directly gives the degree of complexity of the space involved. These profiles that are derived by computer simulation seem to be in very good agreement with experimental data of fluorescence probing in microemulsion and lipid vesicles.

Acknowledgment. We are grateful to Dr. G. Duportail for providing the experimental decay profile. This work was supported by ΠΕΝΕΔ Grant 89EΔ477 (Greek Secretariat of Research and Technology).

References and Notes

(1) Kopelman, R. *J. Stat. Phys.* **1986**, *42*, 185. Kopelman, R. *Science* **1988**, *241*, 1620.
(2) Zana, R. In *Surfactant Solutions, New Methods of Investigation*; Surfactant Science Series; Zana, R., Ed.; Marcel Dekker: New York, 1987; Vol. 22, p 41.
(3) Infetta, P. P.; Gratzel, M.; Thomas, J. K. *J. Phys. Chem.* **1974**, *78*, 19, 90.
(4) Almgren, M.; Lofroth, J.-E.; van Stam, J. *J. Phys. Chem.* **1986**, *90*, 31, 443.
(5) Vanderkooi, J. M.; Callis, J. B. *Biochemistry* **1974**, 13, 4000.
(6) Daems, D.; van den Zegel, M.; Boens, N.; De Schryver, F. C. *Eur. Biophys. J.* **1985**, *12*, 97.
(7) L'Heureux, G. P.; Fragata, M. *J. Photochem. Photobiol.* **1989**, *3*, 53.
(8) Lin, B. M.; Cheung, H. C.; Chen, K. H.; Habercom, M. S. *Biophys. Chem.* **1980**, *12*, 341.
(9) Gehlen, M. H.; Boens, N.; De Schryver, F. C.; Van der Auweraer, M.; Reekmanns, S. *J.* Phys. *Chem.* **1992**, *96*, 5592.
(10) Livesey, A. K.; Brochon, J. C. *Biophys. J.* **1987**, *52*, 693.
(11) Dexter, D. L. *J. Chem. Phys.* **1953**, *21*, 836.
(12) Blumen, A. *Nuovo Cimento* **1981**, *63B*, 50.
(13) Allinger, K.; Blumen, A. *J. Chem. Phys.* **1980**, *72*, 4608.
(14) Blumen, A.; Klafter, J.; Zumofen, G. *Phys. Rev. B* **1983**, *28*, 6112.
(15) Zumofen, G.; Blumen, A. *Chem. Phys. Lett.* **1982**, *88*, 63.
(16) Klafter, J.; Blumen, A. *J. Chem. Phys.* **1984**, *80*, 875.
(17) Stuart, A.; Ord, J. In *Kendall's Advanced Theory of Statistics*; Charles Griffin & Co Ltd.: London, Vol. 1, p 84.
(18) Lianos, P.; Duportail, G. *Eur. Biophys. J.* **1992**, *21*, 29.
(19) Lianos, P.; Modes, S.; Staikos, G.; Brown, W. *Langmuir* **1992**, *8*, 1054.
(20) Lianos, P.; Brochon, J. C.; Tauc, P. *Chem. Phys.* **1993**, *170*, 235.
(21) Alexander, S.; Orbach, R. *J. Phys.* (*Lett*) **1982**, *43*, L-625.
(22) Papoutsi, D.; Lianos, P.; Brown, W. *Langmuir* **1993**, *9*, 663.
(23) Papadimitriou, V.; Xenakis, A.; Lianos, P. *Langmuir* **1993**, *9*, 912.
(24) Argyrakis, P.; Duportail, G.; Lianos, P. *J. Chem. Phys.* **1991**, *95*, 3808.
(25) Duportail, G.; Brochon, J.-G.; Lianos, P. *J. Phys. Chem.* **1992**, *96*, 6, 146.
(26) Duportail, G.; Brochon, J.-G.; Lianos, P. *Biophys. Chem.* **1993**, *45*, 227.
(27) Lianos, P.; Duportail, G. *Biophys. Chem.*, in press.